Journal of Engineering Science and Technology
Vol. 12, No. 12 (2017) 3376 - 3397

SIMULTANEOUS SPACE VECTOR MODULATION DIRECT TORQUE CONTROL OF TWO INDUCTION MOTORS USED IN ELECTRIC VEHICLES BY A NINE-SWITCH INVERTER

A. R. SHAMLOU[1,*], M. R. FEYZI[2], S.TOHIDI[3], M. VALIZADEH[4]

[1, 2, 3] Faculty of Electrical and Computer Engineering, University of Tabriz, Tabriz, Iran
[4]Department of Electrical Engineering, University of Ilam, Ilam, Iran
*Corresponding Author: a.shamlou91@ms.tabrizu.ac.ir

Abstract

In this paper, a novel two output nine switch-inverter is proposed in order to increase the synchronization speed of induction motors used in electric vehicles (EVs) while improving the efficiency and controllability of the system. The number of switches in the proposed inverter is reduced by 25% compared to double six-switch inverters which conventionally used in EVs. The main characteristics of the considered inverter can be noted as follows: sinusoidal input and outputs, unity output power factor, and specifically, low construction cost due to active switch number reduction. The classical direct torque control method causes torque ripple and speed fluctuations. Therefore, in order to increase accuracy and dynamics of drive system, the SVM-DTC method is proposed, leading to less torque ripple and constant switching frequency. The obtained torque ripple is 2% which is less than the existing structures In order to illustrate advantages of the proposed approach, performance of the EVs in the standard cycles is evaluated.

Keywords: Nine switch inverter, EVs, Direct torque control, SVM-DTC.

1. Introduction

In recent years, lack of the fossil fuels and also environmental concerns, lead to the idea that the combustion engines would be a crisis in human lives [1]. Accordingly, a new version of vehicles, named as electric vehicles (EVs), got appeared and widely used. EVs would reduce air pollution, generated greenhouse gases and also the oil consumption [2].

Induction motor is one the most commonly used motors in automobiles [3]. An

Nomenclatures

f_m	Motor reference signal frequencies, Hz
T_0	applying time of zero vectors, s
$T_{Am,\,k}$	First applying time period of motor, s
$T_{Am,\,k+1}$	Second applying time period of motor, s
T_s	Total sampling time, s
V_{refm1}	Reference voltage vector of motor1, V
V_{refm2}	Reference voltage vector of motor2, V

Greek Symbols

Φ_m	Phase of reference voltage signal
θ	angle of voltage vector
ψ	Flux of motor

Abbreviations

DTC	Direct Torque Control
EVs	Electric Vehicles
SVM	Space Vector Modulation

electrical vehicle consists of at least, two induction motors conventionally fed by two independent inverters. This structure makes an EV hard to control [4].

The idea of using one inverter in order to control and drive two induction motors is firstly introduced for a locomotive system in 1984. Considering a locomotive system, the induction motors connected in parallel. Consequently, the independent control of motors seemed to be impossible [5]. On the other hand, it is not neglect able that, dual induction motors driving by a single inverter, leads to reducing the number of converter switches which improves the system performance [6].

As it was mentioned, using one inverter to control dual motors increases the system efficiency. Therefore, the mentioned concept widely studied in the literature with the purpose of performance improving [7-9]. The idea of replacing a five leg inverter with a six leg one is introduced in order to drive a traction motor and a compressor one, simultaneously [7]. In the mentioned system, three legs of the inverter are used to supply the traction motor and the other two legs are responsible for the three terminal two-phase compressor motor. Due to one leg reduction compared with six-leg inverter, the common terminal of two-phase motor is connected to the neutral point of three-phase traction motor.

A five-leg inverter is considered to drive dual three-phase induction motors [8]. However, two phases of each machine are directly connected to four legs of the inverter. Furthermore, the remained phase of each machine should meet the fifth leg. This affects the independent control.

Moreover, the concept of utilizing a four leg inverter in order to drive dual independent motors, is firstly mentioned in 2011 [9]. The mentioned inverter consists of four legs connected to two phases of each motors, separately. On the other hand there are two capacitors connected in series. The remained phase of both motors connected to the neutral point of the capacitors. However, it is

obvious that, achieving an independent controlling approach is also impossible in this case [9].

Moreover, a nine switch inverter is used in order to control dual outputs, simultaneously [10]. The properties of such an inverter can be summarized as: AC form of input and outputs, unity output power factor and more importantly, low price due to the reduction in switch numbers. The proposed converter has only three legs with three switches installed on each. As the middle switch of each leg, is shared by the inverter and also the rectifier, the switch numbers will reduce by 33% and 50% in comparison to the 12 switch back to back VSI and 18 switch matrix converter, respectively.

A multi-machine system is also considered to be controlled utilizing a control method based on direct torque control (DTC) [11]. The DTC based control methods mainly, consist of two separate control loops, the torque and flux control loops. In the torque control loop, firstly, the system overall requirement is specified according to motor torque requirements. Afterwards, the optimum voltage vector is selected. On the other hand, the flux control loop, utilizes a master-slave controlling approach. The proposed method is simulated for a two parallel induction motors and also can be extended to multi-machine systems. However, the mentioned approach causes torque ripple and affects the system performance.

As it was mentioned, the direct torque control approach is known as a novel efficient method in order to control the speed and torque of an induction motor [12]. The electromagnetic torque, stator flux value and also flux vector position are estimated utilizing the inverter input DC voltage and the stator currents. Afterwards, considering the mentioned parameters, the inverter switching commands would be established [13].

Although the direct torque control is an easy to implement technique, the conventional DTC due to its hysteresis controllers, suffers from variable switching frequency and high torque ripple [14]. In order to solve such problems, the SVM-DTC approach is proposed [15]. The principle of proposed approach is to apply the appropriate voltage vectors in order to control the flux and torque. As a consequence, the calculation time increases. However, this is not problematic due to developing of novel digital technologies [16].

In this paper, a two output nine switch inverter is proposed to increase the synchronization speed of the induction motors of an EV. Due to weaknesses of the classic DTC in simultaneously controlling of two induction motors, the SVM-DTC approach is in used. At each moment, by comparing the operating regions and also determining the voltage vector situations, the appropriate voltage vector is calculated and applied to the outputs. This approach, leads to effective and independent control of both the motors, while the installed semiconductors reduced by 25% compared to 12 switches back to back VSI.

The paper is organized as follows: In Section 2, the nine switch inverter structure is discussed. Section 3 presents the basics of the direct torque control method. In section 4, the proposed SVM-DTC approach and its step by step implementation for dual induction motors controlling by a NSI, is presented. Section 5 presents simulation studies. Finally section 6 concludes the findings and contributions of the paper.

2. Dual Induction Motors- Nine Switch Inverter Configuration

Figure 1 illustrates the structure of a three-phase nine-switch inverter (NSI), which combines two three-phase inverters with three common switches. Schematically, this converter has three legs with three switches installed on each of them. However, this structure leads to some kinds of constraints in switching' states. For instant, all of the three switches could not be closed simultaneously, since it would cause the short-circuit occurrence. On other hand, in order to avoid floating the outputs, two switches should be closed at each moment.

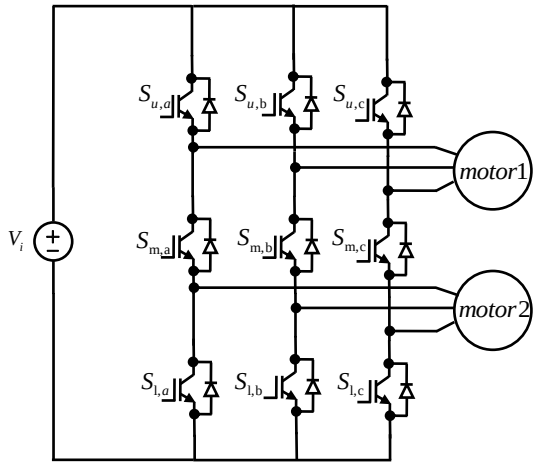

Fig. 1. Nine-switch inverter structure.

In order to control two independent induction motors by a nine-switch inverter, the inverter switches are classified as follows. The upper part, named Inv1, consists of the switches designated S_{ua}, S_{ub}, S_{uc}, S_{ma}, S_{mb} and S_{mc}. On the other hand, the lower part, named Inv2, consists of the switches designated S_{ma}, S_{mb}, S_{mc}, S_{la}, S_{lb} and S_{lc}. Thus, the middle switches are shared by Inv1 and Inv2. Inv1 and Inv2 are responsible for controlling the motor1 and motor2, respectively.

Considering the proposed topology, three different operating conditions are remarkable depending of the motor to be controlled. If driving of motor1 is in the priority, the Inv1 switches will be deterministic. On the other hand, Inv2 switches are responsible for driving motor2. However, the target of this paper is to simultaneously drive both the motors efficiently. Next section describes the Direct Torque Control (DTC) approach due to dual machines control.

3. Simultaneous Direct Torque Control of Two Induction Motors

The idea for the DTC is to apply in alternative active vectors. In order to drive motor1, six active voltage vectors, named V1-V6 are available. On the other hand, active voltage vectors related to motor2 are indicated as V7-V12. Tables 1 and 2 illustrate the selectable voltage vectors of motor1 and motor2, respectively. As evident, by applying a specified voltage vector to one of the motors, the available vectors for other one will be limited.

Table 1. DTC selectable active voltage vectors of motor1.

selectable / selected	V_7	V_8	V_9	V_{10}	V_{11}	V_{12}
V_1	✓	-	-	-	-	-
V_2	✓	✓	✓	-	-	-
V_3	-	-	✓	-	-	-
V_4	-	-	✓	✓	✓	-
V_5	-	-	-	-	✓	-
V_6	✓	-	-	-	✓	✓

Table 2. DTC selectable active voltage vectors of motor2.

selectable / selected	V_1	V_2	V_3	V_4	V_5	V_6
V_7	✓	✓	-	-	-	✓
V_8	-	✓	-	-	-	-
V_9	-	✓	✓	✓	-	-
V_{10}	-	-	-	✓	-	-
V_{11}	-	-	-	✓	✓	✓
V_{12}	-	-	-	-	-	✓

When an EV turns in road, its wheels have different speeds. Consequently, its motors experience different conditions. In other words, the inverter receives two different voltage references simultaneously. As mentioned earlier, in order to drive two independent motors with DTC approach, the upper and lower three switches are triggered to control the upper and lower motors, respectively. Due to active vector limitations, inappropriate voltages may be sent to the related motors. However, this leads to the torque waveform distortion and motor speed fluctuation. Consequently, the conventional DTC approach faces significant weaknesses in simultaneous control of two independent motors. In order to overcome such problems, the space vector modulation (SVM) DTC approach is proposed in this paper. The proposed method is capable of solving mentioned problems.

4. Proposed SVM-DTC Approach in Order to Dual Motor Control

The proposed control scheme of induction motors associated to the nine switch inverter is presented in Fig. 2.

In this case, the electromagnetic torque and the stator flux are controlled directly in closed-loops. Hence, an accurate estimation of these parameters is required. As illustrated in Fig. 2, the estimated magnitude of torque and stator flux go to PI controller. The PI controller outputs are the stator voltage references. Afterwards, the reference parameters, named u^*_{ds} and u^*_{qs} are applied to the static reference frame ($\alpha\beta$). Finally the SVM block receives the signals. As mentioned before, the SVM approach, due to its reliefs, improves the DTC performance. In the next step, the SVM block and its operation is elaborated.

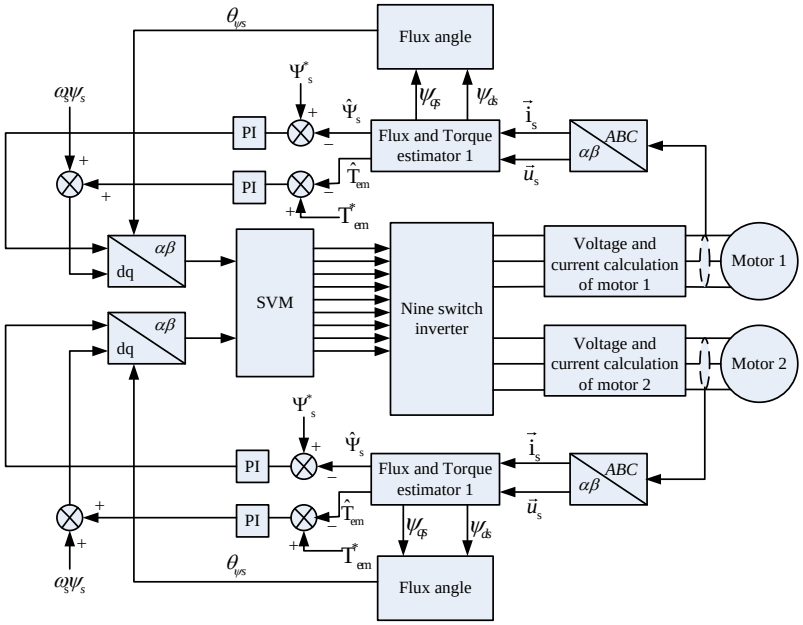

Fig. 2. Proposed SVM-DTC control diagram.

4.1. SVM block

As it is obvious, each leg of a nine switch inverter has eight different ON–OFF states. As it was mentioned, at least, two switches should be closed at each moment in order to avoid floating the outputs. Moreover, it is obvious that all three switches cannot be closed at the same time due to avoid DC bus short-circuit. Therefore, only three on-off states are possible. Table 3 illustrates these circumstances called (-1), (0) and (1). In Table 3, k denotes to the name of legs (1, 2 or 3).further, u, m and l represent the upper, middle and lower switches, respectively.

Attending three possible states for each leg, there are 27 various states for the NSI. Table 4 shows the possible states, called NSI vector.

The NSI vectors can be divided into four groups:

1- motor1-active vectors: The upper motor receives active vectors, but the lower motor receives zero vectors.

2- motor2-active vectors: The lower motor receives active vectors, but the upper motor receives zero vectors.

3- both-active vectors: Both the motors receive active state.

4- zero state: Both the motors receives zero vectors.

Table 4 illustrates switching vectors of NSI and on-off position of each of nine switches.

Moreover, Fig. 3, illustrates the space presentation of the NSI vectors according to Table 3 and Table 4.

Table 3. Switches on- off position.

	$S_{u,k}$	$S_{m,k}$	$S_{l,k}$
-1	on	off	on
1	on	on	off
0	off	on	on

Table 4. Switching vectors of NSI.

Vector	Leg 1	Leg 2	Leg 3	Type
$V_{1,0}$	-1	0	0	Motor 1 active
$V_{2,0}$	-1	-1	0	
$V_{3,0}$	0	-1	0	
$V_{4,0}$	0	-1	-1	
$V_{5,0}$	0	0	-1	
$V_{6,0}$	-1	0	-1	
$V_{0,7}$	1	-1	-1	Motor2 active
$V_{0,8}$	1	1	-1	
$V_{0,9}$	-1	1	-1	
$V_{0,10}$	-1	1	1	
$V_{0,11}$	-1	-1	1	
$V_{0,12}$	1	-1	1	
$V_{1,7}$	1	0	0	Both active
$V_{2,8}$	1	1	0	
$V_{3,9}$	0	1	0	
$V_{4,10}$	0	1	1	
$V_{5,11}$	0	0	1	
$V_{6,12}$	1	0	1	
$V_{2,7}$	1	-1	0	
$V_{2,9}$	-1	1	0	
$V_{4,9}$	0	1	-1	
$V_{4,11}$	0	-1	1	
$V_{6,11}$	-1	0	1	
$V_{6,7}$	1	0	-1	
V_{13}	-1	-1	-1	zero
V_{14}	0	0	0	
V_{15}	1	1	1	

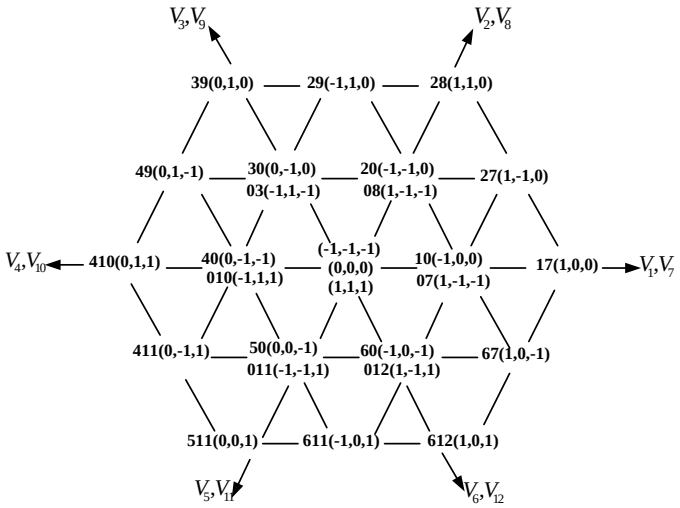

Fig. 3. Switching vectors of NSI.

In this paper, the reference signals, named V_{ref1}, V_{ref2}, determine how to apply the active and zero vectors to the under control motors. The mentioned reference signals are specified as follows.

$$\vec{V}_{refm1} = V_{refm1} \angle \alpha_{m1} \tag{1}$$

$$\vec{V}_{refm2} = V_{refm2} \angle \alpha_{m2} \tag{2}$$

$$\alpha_{m1} = 2\pi f_{m1} t + \phi_{m1} \tag{3}$$

$$\alpha_{m2} = 2\pi f_{m2} t + \phi_{m2} \tag{4}$$

where f_{m1} and f_{m2} are the motor1 and motor2 reference signal frequencies, respectively. Moreover, Φ_{m1} and Φ_{m2} represent the phase of above mentioned reference signals.

It is noteworthy to note that the reference signal positions in the space vector diagram determine the appropriate switching vectors. In the proposed control method, it is preferred to apply active vectors to both the motors. In addition, in an appropriate switching strategy, switching numbers from one state to another state should be minimal. As illustrated in Fig. 4, the space vector diagram is divided into six distinct sections.

However, selecting an optimal switching interval depends on the location of space vector diagram of reference vectors. If the phase difference between reference vectors is less than 60 degrees, the references are assumed to be in the same section. Thereupon the active vectors can be applied to both the outputs. On the other hand, if such phase difference is less than 120 degrees, references are in vicinity. Active vectors also can be applied to both the outputs in this case. As a

result, the identical vectors can be applied for the reference with the regional difference less than 3.

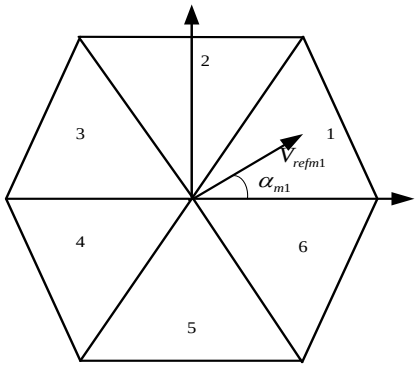

Fig. 4. Space vector classification.

4.2. SVM switching in far sections

As mentioned earlier, it is difficult to control two induction motors of an electric vehicle when the voltage references are in sections with the phase difference more than 120 degrees. In order to overcome the dilemma of receiving different vectors, the proposed approach in this paper is to half the switching period. However, in the proposed approach, in the first half period, motor1 receives active vector while motor2 receives zero one. On the other hand, during the second half period, motor2 gets the active vector and the zero vector delivers to motor1. Tables 5 and 6 illustrate the proposed SVM switching vector sequence to be applied to the NSI. An important point about the following tables is to make sure that the sum of the both table terms should be equal to zero.

Table 5. SVM switching vector sequence in the first half period.

V_Z	V_{Am1}	V_{Am1}	V_{Am1}	V_{Am1}	V_Z
$\frac{T_0}{4}$	$\frac{T_1}{2}$	$\frac{T_2}{2}$	$\frac{T_2}{2}$	$\frac{T_1}{2}$	$\frac{T_0}{4}$

Table 6. SVM switching vector sequence in the second half period.

V_Z	V_{Am2}	V_{Am2}	V_{Am2}	V_{Am2}	V_Z
$\frac{T_0}{4}$	$\frac{T_3}{2}$	$\frac{T_4}{2}$	$\frac{T_4}{2}$	$\frac{T_3}{2}$	$\frac{T_0}{4}$

Moreover, the voltage vectors applying order and time intervals are provided in Tables 7 and 8. As outlined above, minimizing the switching times is the target. However, the minimum switching number occurs when the vectors $V_{m1,\ 1}$ and $V_{m1,\ 2}$ are selected according to Table 7. $V_{m2,\ 1}$ and $V_{m2,\ 2}$ should be also selected confirming to Table 8. It should be noted that, $V_{m1,\ 1}$ and $V_{m1,\ 2}$ are two adjacent voltage vectors of motor1.

Table 7. SVM switching plan for motor1 considering reduced switching number in the first half period.

V_{refm1} **in 1th, 3th, 5th section**					
V_{13}	$V_{Am1,2}$	$V_{Am1,1}$	$V_{Am1,1}$	$V_{Am1,2}$	V_{13}
$\frac{T_0}{4}$	$\frac{T_2}{2}$	$\frac{T_1}{2}$	$\frac{T_1}{2}$	$\frac{T_2}{2}$	$\frac{T_0}{4}$
V_{refm1} **in 2th,4th, 6th section**					
V_{13}	$V_{Am1,1}$	$V_{Am1,2}$	$V_{Am1,2}$	$V_{Am1,1}$	V_{13}
$\frac{T_0}{4}$	$\frac{T_1}{2}$	$\frac{T_2}{2}$	$\frac{T_2}{2}$	$\frac{T_1}{2}$	$\frac{T_0}{4}$

Table 8. SVM switching plan for Motor2 considering reduced switching number in the second half period.

V_{refm2} **in 1th, 3th, 5th section**					
V_{13}	$V_{Am2,1}$	$V_{Am2,2}$	$V_{Am2,2}$	$V_{Am2,1}$	V_{13}
$\frac{T_0}{4}$	$\frac{T_3}{2}$	$\frac{T_4}{2}$	$\frac{T_4}{2}$	$\frac{T_3}{2}$	$\frac{T_0}{4}$
V_{refm2} **in 2th,4th, 6th section**					
V_{13}	$V_{Am2,2}$	$V_{Am2,1}$	$V_{Am2,1}$	$V_{Am2,2}$	V_{13}
$\frac{T_0}{4}$	$\frac{T_4}{2}$	$\frac{T_3}{2}$	$\frac{T_3}{2}$	$\frac{T_4}{2}$	$\frac{T_0}{4}$

According to Tables 7 and 8, if the zero vector, V_{13} stands between the first and second active vectors, the minimum switching number will be required. On the other hand, the use of zero vectors (V_{14} and V_{15}) increases the switching frequency.

It should be noted that the most important part of the SVM technique is calculating the applying time of active and zero vectors. Since the total sampling time, T_s, is short, the reference vectors of motors could be assumed constant during T_s . Considering Tables 7 and 8, during the sampling time, the voltage of reference vectors can be calculated as follows.

$$\frac{\int_{T_s} \vec{V}_{refm1}}{T_s} = \frac{\int_{T_{Am1,k}} \vec{V}_{Am1,k}\, dt + \int_{T_{Am1,k+1}} \vec{V}_{Am1,k+1}\, dt}{T_s} + \frac{\int_{T_{Am2,k'}} \vec{V}_{Am2,k'}\, dt + \int_{T_{Am2,k'+1}} \vec{V}_{Am2,k'+1}\, dt + \int_{T_0} \vec{V}_{13}}{T_s} \quad (5)$$

$$\frac{\int_{0}^{T_s} \vec{V}_{refm2}}{T_s} = \frac{\int_{0}^{T_{Am1,k}} \vec{V}_{Am1,k}\, dt + \int_{0}^{T_{Am1,k+1}} \vec{V}_{Am1,k+1}\, dt}{T_s} + \frac{\int_{0}^{T_{Am2,k'}} \vec{V}_{Am2,k'}\, dt + \int_{0}^{T_{Am2,k'+1}} \vec{V}_{Am2,k'+1}\, dt + \int_{0}^{T_0} \vec{V}_{13}}{T_s} \tag{6}$$

where $V_{Am1,k}$ and $V_{Am1,k+1}$ are the first and second active vectors of motor1 in the k^{th} section. On the other hand, $V_{Am2,\,k'}$ and $V_{Am2,\,k'+1}$ are the first and second active vectors of motor2 in the k'^{th} section, respectively. Moreover, $T_{Am1,\,k}$ and $T_{Am1,\,k+1}$ are the first and second applying time period of Motor1 in the k^{th} section. Also, $T_{Am2,\,k'}$ and $T_{Am2,\,k'+1}$ are the first and second applying time period of Motor2 in the k'^{th} section, respectively. Eqs. (5) and (6) can also be stated as:

$$T_s\ \vec{V}_{refm1} = \vec{V}_{Am1,k}\, T_{Am1,k} + \vec{V}_{Am1,k+1}\, T_{Am1,k+1} \tag{7}$$

$$T_s\ \vec{V}_{refm2} = \vec{V}_{Am2,k'}\, T_{Am2,k'} + \vec{V}_{Am2,k'+1}\, T_{Am2,k'+1} \tag{8}$$

Decomposing (7) into the real and imaginary parts, yields:

$$\begin{aligned} T_s \begin{bmatrix} V_d \\ V_q \end{bmatrix} &= \frac{2}{3} V_i\, T_{Am1,k} \begin{bmatrix} \cos\frac{(k-1)\pi}{3} \\ \sin\frac{(k-1)\pi}{3} \end{bmatrix} + \frac{2}{3} V_i\, T_{Am1,k+1} \begin{bmatrix} \cos\frac{k\pi}{3} \\ \sin\frac{k\pi}{3} \end{bmatrix} \\ &= \frac{2}{3} V_i \begin{bmatrix} \cos\frac{(k-1)\pi}{3} & \cos\frac{k\pi}{3} \\ \sin\frac{(k-1)\pi}{3} & \sin\frac{k\pi}{3} \end{bmatrix} \begin{bmatrix} T_{Am1,k} \\ T_{Am1,k+1} \end{bmatrix} \end{aligned} \tag{9}$$

Solving (9) obtains the following equation:

$$\begin{bmatrix} T_{Am1,k} \\ T_{Am1,k+1} \end{bmatrix} = \sqrt{3}\frac{T_s}{V_i} \begin{bmatrix} \sin\frac{k\pi}{3} & -\cos\frac{k\pi}{3} \\ -\sin\frac{(k-1)\pi}{3} & \cos\frac{(k-1)\pi}{3} \end{bmatrix} \begin{bmatrix} V_d \\ V_q \end{bmatrix} \tag{10}$$

On the other hand, Eq. (1) could be presented as:

$$\begin{aligned} \vec{V}_{refm1} &= V_{refm1} \angle \alpha_{m1} \\ &= V_d + jV_q \\ &= V_{refm1} \cos\alpha_{m1} + jV_{refm1} \sin\alpha_{m1} \end{aligned} \tag{11}$$

Considering Eqs. (10) and (11), the following equation is obtained.

$$\begin{bmatrix} T_{Am1,k} \\ T_{Am1,k+1} \end{bmatrix} = \sqrt{3}\frac{T_s V_{refm1}}{V_i}\begin{bmatrix} \sin\frac{k\pi}{3} & -\cos\frac{k\pi}{3} \\ -\sin\frac{(k-1)\pi}{3} & \cos\frac{(k-1)\pi}{3} \end{bmatrix}\begin{bmatrix} \cos\alpha_{m1} \\ \sin\alpha_{m1} \end{bmatrix}$$
$$= \sqrt{3}\frac{TV_{refm1}}{V_i}\begin{bmatrix} \sin\left(\frac{k\pi}{3}-\alpha_{m1}\right) \\ \sin\left(\alpha_{m1}-\frac{(k-1)\pi}{3}\right) \end{bmatrix} \quad (12)$$

Similar to the mentioned process, Eq. (8) is obtained.

$$\begin{bmatrix} T_{Am2,k'} \\ T_{Am2,k'+1} \end{bmatrix} = \sqrt{3}\frac{T_s V_{refm2}}{V_i}\begin{bmatrix} \sin\frac{k'\pi}{3} & -\cos\frac{k'\pi}{3} \\ -\sin\frac{(k'-1)\pi}{3} & \cos\frac{(k'-1)\pi}{3} \end{bmatrix}\begin{bmatrix} \cos\alpha_{m2} \\ \sin\alpha_{m2} \end{bmatrix}$$
$$= \sqrt{3}\frac{TV_{refm2}}{V_i}\begin{bmatrix} \sin\left(\frac{k'\pi}{3}-\alpha_{m2}\right) \\ \sin\left(\alpha_{m2}-\frac{(k'-1)\pi}{3}\right) \end{bmatrix} \quad (13)$$

Particularly, if both the reference vectors stand in the first section:

$$T_1 = T_{Am1,1} = \sqrt{3}\frac{T_s V_{refm1}}{V_i}\sin\left(\frac{\pi}{3}-\alpha_{m1}\right) \quad (14)$$

$$T_2 = T_{Am1,2} = \sqrt{3}\frac{T_s V_{refm1}}{V_i}\sin(\alpha_{m1}) \quad (15)$$

$$T_3 = T_{Am2,1} = \sqrt{3}\frac{T_s V_{refm2}}{V_i}\sin\left(\frac{\pi}{3}-\alpha_{m2}\right) \quad (16)$$

$$T_4 = T_{Am2,2} = \sqrt{3}\frac{T_s V_{refm2}}{V_i}\sin(\alpha_{m2}) \quad (17)$$

$$T_0 = T_s - T_1 - T_2 - T_3 - T_4 \quad (18)$$

where T_1 and T_2 are the applying time intervals of motor1 active vectors. On the other hand, T_3 and T_4 present the applying time periods of motor2 active vectors. Further, T_0 is the applying time of zero vectors and T is the total switching time.

4.3. SVM switching in adjacent sections

When the phase difference between the reference signals of motor1 and motor2 is less than 120 degrees, two references are adjacent. Accordingly, concurrent active vectors could be applied. By considering two independent SVM blocks for

motor1 and motor2, and comparing the time periods T1, T2, T3 and T4, the applied switching sequence will be specified. If motor1 and motor2 stand in the fourth and third sections, respectively, the NSI switching vectors should be implemented as shown in Fig 5. Moreover, Fig. 6 indicates the block diagram of such case. Furthermore, switching vectors and time intervals of the understudied case are presented in Table 9.

In all the switching intervals proposed in Table 9, T_0 equal to $T_{Z1}+T_{Z2}$. Values of T_{Z1} and T_{Z2} are set to be $T_0/2$ compared to the different conditions, the amount of T_0 time varies.

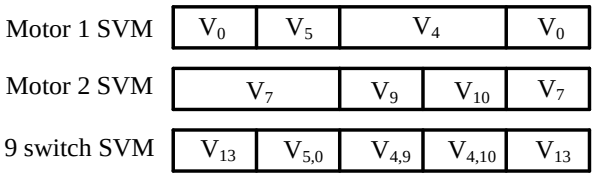

Fig. 5. Switching vectors in adjacent sections.

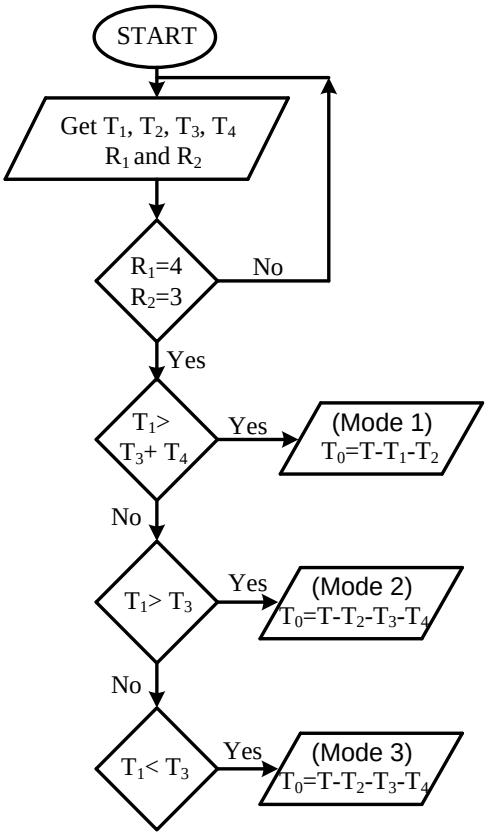

Fig. 6. Algorithm of applying active vectors in adjacent sections.

Table 9. Switching vectors and time intervals in adjacent sections.

Mode	Vectors R_1=4, R_2=3	Time interval
1	$V_{13},V_{5,0},V_{4,0},V_{4,9},V_{4,10},V_{13}$	$T_{z1},T_2,T_1\text{-}T_3\text{-}T_4,T_3,T_4,T_{z2}$
2	$V_{13},V_{5,0},V_{4,9},V_{4,10},V_{0,4},V_{13}T_{z1},T_2,T_3,T_1\text{-}T_3,T_3\text{+}T_4\text{-}T_1,T_{z2}$	
3	$V_{13},V_{5,0},V_{4,9},V_{0,3},V_{0,4},V_{13}$	$T_{z1},T_2,T_1,T_3\text{-}T_1,T_4,T_{z2}$

4.4. SVM switching in the same section

If the phase difference between the reference signals is less than 60 degrees, both reference signals can be assumed in the same section. In this case, two active vectors can be used for both the outputs. Table 10 presents switching vectors and time intervals when both the references stand in the third section. In comparison to the switching in the adjacent sections, switching in the same section provides higher possibility to apply active vectors in both the outputs. However, in a straight road, due to the same state of the EV wheels, switching process often occurs in the same sections.

Table 10. Switching vectors and V_{ref1} and V_{ref2} time intervals in the third section.

Mode	Vectors R_1=3, R_2=3	Time interval
$T_1+T_2>T_3+T_4,\ T_2>T_3+T_4$	$V_{13},V_{3,0},V_{4,0},V_{4,9},V_{4,10},V_{13}$	$T_{z1},T_1,T_2\text{-}T_3\text{-}T_4,T_3,T_4,T_{z2}$
$T_1+T_2>T_3+T_4,$ $T_4<T_2<T_3+T_4$	$V_{13},V_{3,0},V_{3,9},V_{4,9},V_{4,10},V_{13}$	$T_{Z1},T_1+T_2\text{-}T_3\text{-}T_4,T_3+T_4\text{-}T_2,T_2\text{-}T_4,T_4,T_{z2}$
$T_1+T_2>T_3+T_4,\ T_4>T_2$	$V_{13},V_{3,0},V_{3,9},V_{4,10},V_{0,10},V_{13}$	$T_{z1},T_1\text{-}T_3,T_3,T_2,T_4\text{-}T_2,T_{z2}$
$T_1+T_2<T_3+T_4,\ T_3>T_1+T_2$	$V_{13},V_{3,9},V_{4,9},V_{0,9},V_{0,10},V_{13}$	$T_{z1},T_1,T_2,T_3\text{-}T_1\text{-}T_2,T_4,T_{Z2}$
$T_1+T_2<T_3+T_4,$ $T_1<T_3<T_1+T_2$	$V_{13},V_{3,9},V_{4,9},V_{4,10},V_{0,10},V_{13}$	$T_{z1},T_1,T_3\text{-}T_1,T_1+T_2\text{-}T_3,T_3+T_4\text{-}T_1\text{-}T_2,T_{z2}$
$T_1+T_2<T_3+T_4,\ T_1>T_3$	$V_{13},V_{3,0},V_{3,9},V_{4,10},V_{0,10},V_{13}$	$T_{z1},T_1\text{-}T_3,T_3,T_2,T_4\text{-}T_2,T_{z2}$

5. Simulation and Discussion

In this paper, in order to evaluate the performance of the EV, the standard driving cycles of New York City (NYCCDS) and (UN/ECE) are considered.

5.1. Simulation analyses in NYCCDS cycle

NYCCDS cycle is 1.18 miles (1.899 meters). The average speed in this test is 7.1 mile (11.43 km) per hour and the maximum speed is equal to 44.57 km per hour. The test takes 598 seconds. The wheel diameter of the simulated vehicle is equal to 50cm. In order to illustrate the fast dynamic response of the drive system, NYCCDS speed varies every 30 seconds. However, simulation results clarify that the proposed drive technique efficiently response to the alterations twenty times

faster than NYCCDS cycle changes. Figure 7 illustrates the EV speed in the NYCCDS driving cycle. As it is clear, vehicle drive system works well for large changes of speed.

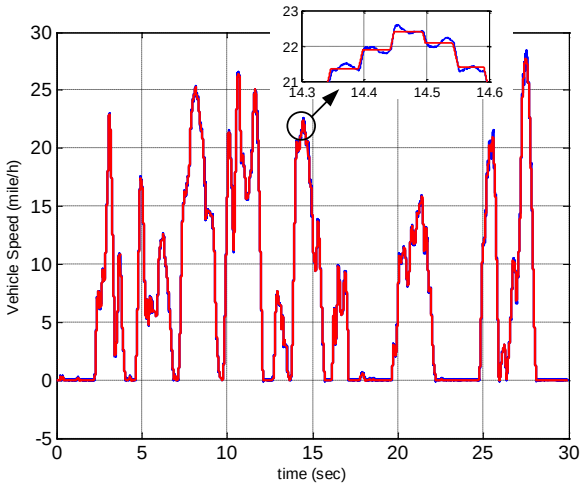

Fig. 7. Vehicle speed curve with NYCCDS driving cycle.

5.2. Simulation analyses in UN/ECE cycle

The UN/ECE cycle is also studied in this paper. The mentioned cycle is designed based on traffic conditions of Paris and Rome. Its specifications are completely different from the New York cycle. This cycle is also known as the European cycle. However, low speed and low engine load are the main features of this cycle. The total time of this test is 195 seconds and the total distance is 994 meters. Moreover, the average speed is 18.35 Km/hour. Figure 8 illustrates the EV speed in the standard European cycle.

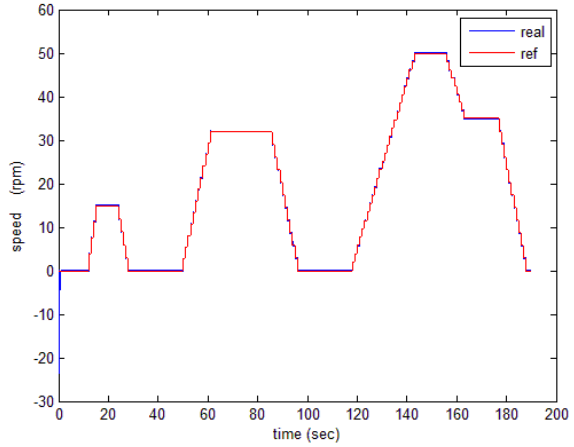

Fig. 8. Speed curve of the vehicle with UN/ECE cycle.

5.3. Turning conditions

In this section, capability of the nine switch inverter and the proposed control method in turning left and right is evaluated. The specification of the studied EV and its electric motors are provided in Table 11.

In this section, the traveled speed curve is considered as follows. Firstly, speeds of both motors increase up to 350 rpm. Afterwards, the vehicle turns left. In order to achieve safe operation, the speed of both motors should be reduced. Consequently, the right and left motor speeds decreases to 340 and 310 rpm, respectively. In the end of the curve, both the motors, again, speed up to 350 rpm. After a 0.5 second, the car turns right. Under this conditions, speeds of the left and right motors decrease to 340 and 310 rpm, respectively. Finally, both the motors speed up to 400 rpm. Figures 9 and 10 illustrate the speed variations of the right and left motors, respectively. Vehicle drive system follow applied reference speed very well. Speed of motors change from each other independently. Both motors track applied reference speed without distortion.

Figure 11 illustrates the efficiency of the motors confronting various speeds. As it is obvious, efficiency of the motor 1 is higher than motor 2.

In order to evaluate the torque ripple and the torque dynamic response of induction motors used in EV and controlled by SVM-DTC, the system response to a step change of reference torque is shown in Fig. 12.

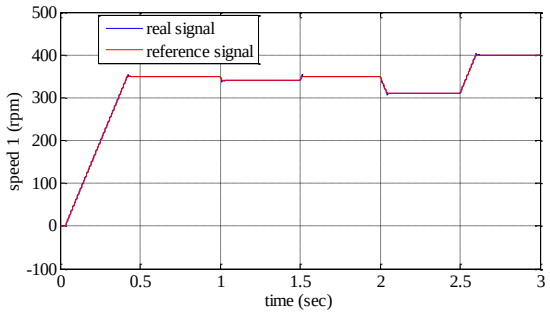

Fig. 9. Right motor speed curve under turning conditions.

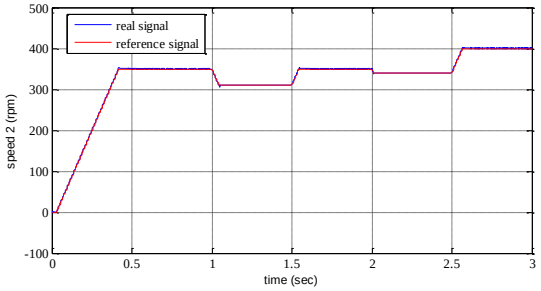

Fig. 10. Left motor speed curve under turning conditions.

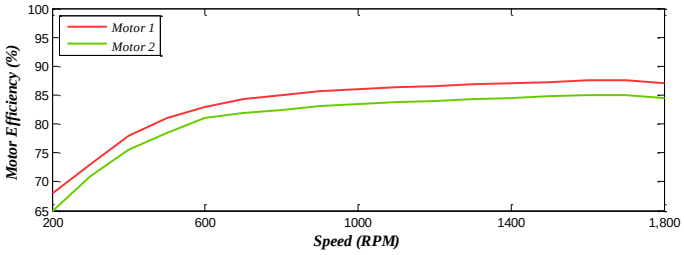

Fig. 11. Motor efficiencies confronting various speeds.

Table 11. Electric vehicle and installed induction motors specifications.

Parameter	Value
Length	4 m
Width	2 m
Height	1 m
Wheelbase	2.5 m
Weight	240 kg
Aerodynamic drag coefficient	0.13
Rolling resistance coefficient	0.006
Number of wheels	Two in front and two in the rear
Rotational inertia	1.15 kgm^2
Wheel radius	0.28 m
Induction motor	2 kW, 380 V, p = 2, 20 Nm, 50 Hz
Rotor resistance	1.82 Ω
Rotor inductance	0.1568 H
Stator resistance	1.2 Ω
Stator inductance	0.1557 H
Mutual inductance	0.158 H
Moment of inertial	0.071 kgm^2

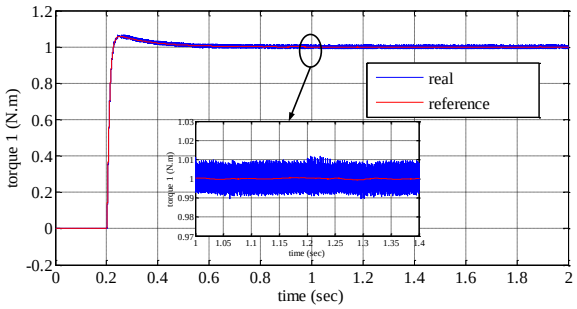

Fig. 12. Torque Step Response in SVM-DTC Approach.

According to Fig. 12, the pick to pick torque ripple is 2%. In addition, the torque step response is compared with the results in the literature [17-19]. The

comparison results are provided in Table 12. As evident, the proposed method leads to significant reduction of torque ripple.

Table 12. Comparison of torque ripple between different control methods.

Torque Ripple	Method	Reference
4%	DTC	[16]
3.4%	New version of DTC	[17]
3.5%	Vector control+DTC	[18]
2%	Proposed Method	

In order to evaluate the transient and steady state behavior of an induction motor, the flux circular path analysis is considered. To achieve this goal, the mentioned curves are provided in Fig. 13 and 14. According to Fig. 13, the flux of motor1 increases from zero and reaches the final value of 0.8 Wb. Fig. 15 and 16 also show the 3 phase currents of motor1 and motor2 during straight road.

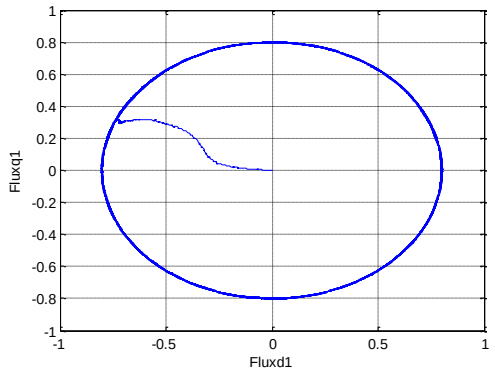

Fig. 13. Motor1 Flux Circle Curve.

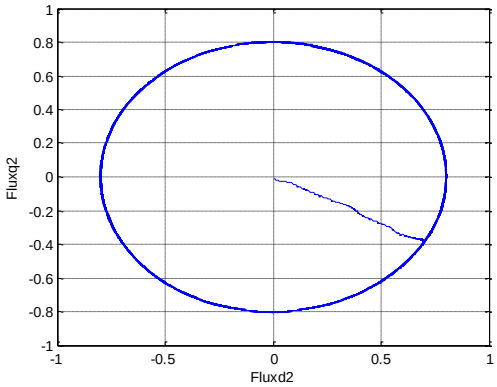

Fig. 14. Motor2 Flux Circle Curve.

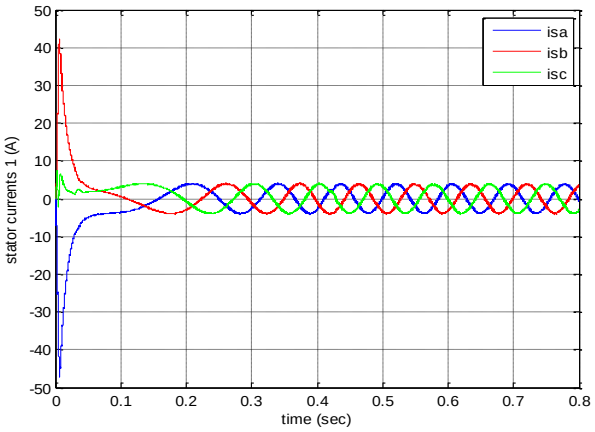

Fig. 15. Motor1 Three-Phase Current.

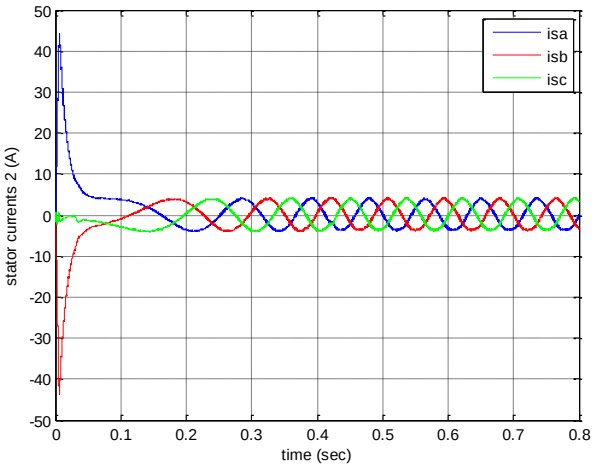

Fig. 16. Motor2 Three-Phase Current.

5.4. Different speed references of motors

In this section, a specific analysis is considered. It should be noted that in a conventional EV, the speed difference of motors is always less than 250 rpm. Hence, the speed difference of two induction motors increases up to 500 rpm. Figures 17 and 18 show the reference and actual speed values of two motors. As evident, although there is difference between the speed reference values, two motors track the reference speeds very well. This means capability of the proposed control scheme to satisfy EV requirements.

However, the proposed control method can be implemented not only in EV control system, but also it can be used as a drive of other systems which need similar operation. It is noteworthy that, none of the previous studies published in literature has the capability to handle the abovementioned conditions.

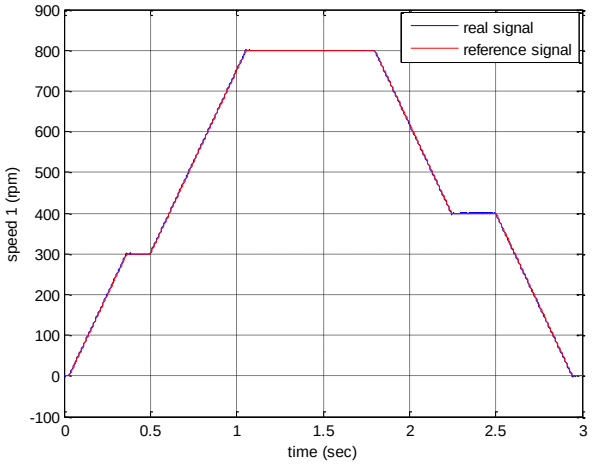

Fig. 17. Reference speed and rotation speed of motor1.

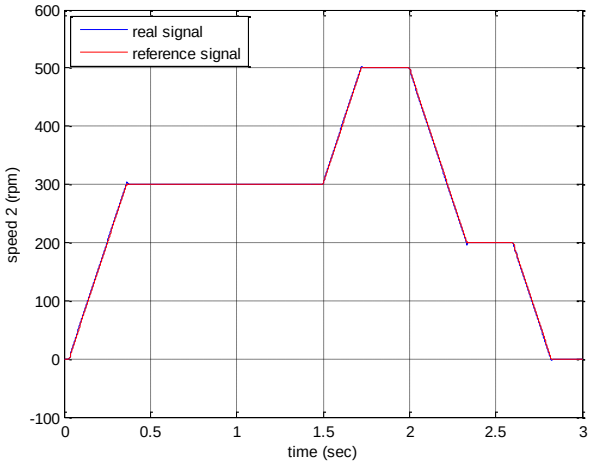

Fig. 18. Reference speed and rotation speed of motor2.

6. Conclusion

In this paper, a two output inverter is proposed to control two induction motors of electric vehicles simultaneously. The following conclusions can be drawn from this study.

- The proposed nine switch inverter improves synchronous performance of the motors which are mechanically decoupled.
- This leads to reduction of the semiconductor switch numbers from 12 to 9.
- The proposed method is suitable for application in electric vehicles.

- The proposed control structure significantly reduces torque ripple and improves the response speed. The obtained torque ripple is 2% which is less than the existing structures.
- The proposed drive system leads to reduction of mechanical stress and hence, enhancement of the life time of the system.
- Cost of inverter reduces due to reduction of switches.
- It is not possible to control both of motors fully independent at every moment and one of motors controls better than other in some moments of time.

References

1. Gasbaoui, B.; Chaker, A.; Laoufi, A.; Allaoua, B.; and Nasri, A. (2011). The efficiency of direct torque control for electric vehicle behavior improvement. *Serbian Journal of Electrical Engineering*, 8(2), 127-146.
2. Green, R.C.; Wang, L.; and Alam, M. (2011). The impact of plug-in hybrid electric vehicles on distribution networks: A review and outlook. *Renewable and Sustainable Energy Reviews*, 15(1), 544-553.
3. Arif, A.; Betka, A.; and Guettaf, A. (2010). Improvement the DTC system for electric vehicles induction motors. *Serbian Journal of Electrical Engineering*, 7(2), 149-165.
4. Moazen, M.; and Sharifian, M.B. (2014). Electric differential for an electric vehicle with four independent driven motors and four wheels steering ability using improved fictitious master synchronization strategy. *Journal of Operation and Automation in Power Engineering*, 2(2), 141-150.
5. Skudenly, H.C.; and Weinhardt, M. (1984). An investigation of the dynamic response of two induction motors in a locomotive truck fed by a common inverter. *IEEE Transactions on Industry Applications*, IA-20(1), 173-179.
6. Babaei, E.; and Laali, S. (2014). Reduction the number of power electronic devices of a cascaded multilevel inverter based on new general topology. *Journal of Operation and Automation in Power Engineering*, 2(2), 81-90.
7. Su, G.J.; and Hsu, J.S. (2006). A five-leg inverter for driving a traction motor and a compressor motor. *IEEE Transactions on Power Electronics*, 21(3), 687-692.
8. Jones, M.; Vukosavic, S.; Dujic, D.; Levi, E.; and Wright, P. (2008). Five-leg inverter PWM technique for reduced switch count two-motor constant power applications. *IET Electric Power Applications*, 2(5), 275-287.
9. Matsuse, K.; Kezuka, N.; and Oka, K. (2011). Characteristics of independent two induction motor drives fed by a four-leg inverter. *IEEE Transactions on Industry Applications*, 47(5), 2125-2134.
10. Liu, C.; Wu, B.; Zargari, N.R.; Xu, D.; and Wang, J. (2009). A novel three-phase three-leg ac/ac converter using nine IGBTs. *Power Electronics, IEEE Transactions on*, 24(5), 1151-1160.
11. Mohktari, H.; and Abdollah, A. (2007). A new multi-machine control system based on Direct Torque Control algorithm. *International Conference on Power Electronics, ICPE'07. 7th*, IEEE. Seoul, Korea, 33-34.

12. Kazmierkowski, M.P.; Franquelo, L.G.; Rodriguez, J.; Perez, M.A.; and Leon, J.I. (2011). High-performance motor drives. *Industrial Electronics Magazine, IEEE*, 5(3), 6-26.
13. Jidin, A.; Idris, N.R.N.; Yatim, A.H.M.; Sutikno, T.; and Elbuluk, M.E. (2011). Simple dynamic overmodulation strategy for fast torque control in DTC of induction machines with constant-switching-frequency controller. *IEEE Transactions on Industry Applications*, 47(5), 2283-2291.
14. Sutikno, T; Idris, N.R.N.; and Jidin, A. (2014). A review of direct torque control of induction motors for sustainable reliability and energy efficient drives. *Renewable and Sustainable Energy Reviews*, 32, 548-558.
15. Oriti, G.; and Julian, A.L. (2011). Three-phase VSI with FPGA-based multisampled space vector modulation. *IEEE Transactions on Industry Applications*, 47(4), 1813-1820.
16. Vasudevan, M.; Arumugam, R.; and Paramasivam, S. (2006). Development of torque and flux ripple minimization algorithm for direct torque control of induction motor drive. *Electrical Engineering*, 89(1), 41-51.
17. Zaid, S.; Mahgoub, O.; and El-Metwally, K. (2010). Implementation of a new fast direct torque control algorithm for induction motor drives. *IET Electric Power Applications*, 4(5), 305-313.
18. Vaez-Zadeh, S.; and Jalali, E. (2007). Combined vector control and direct torque control method for high performance induction motor drives. *Energy conversion and management*, 48(12), 3095-3101.